Supporting information

Probing Lewis Acid-Base Interactions in Single-Molecule Junctions

Xunshan Liu,[a] Xiaohui Li,[b] Sara Sangtarash, *[c] Hatef Sadeghi,[c] Silvio Decurtins,[a] Robert Häner, [a] Wenjing Hong,*[b] Colin J. Lambert*[c] and Shi-Xia Liu*[a]

[a]Department of Chemistry and Biochemistry, University of Bern, Freiestrasse 3, CH-3012 Bern, Switzerland

[b]Department of Chemical and Biochemical Engineering, College of Chemistry and Chemical Engineering, Xiamen University, Xiamen 361005, China

[c]Quantum Technology Centre, Physics Department, Lancaster University, Lancaster LA1 4YB, UK

* whong@xmu.edu.cn; c.lambert@lancaster.ac.uk; s.sangtarash@lancaster.ac.uk; liu@dcb.unibe.ch.

1. Synthesis and characterization of the target compound 1

S-4-iodophenyl ethanethioate,[1] and 1,4-bis(diethynyl)-2,5-bis(dimesitylboryl) benzene[2] were synthesized according to published procedures. All chemicals and solvents were purchased from commercial sources and were used without further purification. The target compound **1** has been fully characterized. Its NMR spectroscopic and high-resolution mass spectrometric data are consistent with its proposed structure. ^{1}H and ^{13}C NMR spectra were recorded on a Bruker Avance 300 spectrometer at 300 and 75.5 MHz, respectively. Chemical shifts are reported in parts per million (ppm) and are referenced to the residual solvent peak ($CDCl_3$, ^{1}H = 7.26 ppm; ^{13}C = 77.16 ppm). Coupling constants (*J*) are given in hertz (Hz) and are quoted to the nearest 0.5 Hz. Peak multiplicities are described in the following way: s, singlet; d, doublet. High-resolution Mass spectrum (HRMS) was recorded with an Auto Spec Q spectrometer in ESI (electrospray ionization) mode.

Microwave reactions was conducted using the Biotage Initiator Eight EXP microwave apparatus and the corresponding vials. The reaction was carried out in the vial (20 mL)

sealed with a septum, under magnetic stirring. The temperature of the reaction mixture was monitored using a calibrated infrared temperature control mounted under the reaction vial.

Synthesis of compound 1. A mixture of *S*-4-iodophenyl ethanethioate (64 mg, 0.21 mmol), 1,4-bis(diethynyl)-2,5-bis(dimesitylboryl)benzene (60 mg, 0.1 mmol), CuI (2 mg, 0.01 mmol) and $Pd(PPh_3)_4$ (6 mg, 0.005 mmol) in Et_3N (7 mL) in a 20 mL vial was purged with N_2 for 15 min. The resulting mixture was subjected to microwave irradiation by pre-stirring for 1 min, and reacted at 50 °C for 8 h. After cooling to room temperature, the solvent was removed in vacuum. The crude product was purified on silica gel chromatography using a mixture of hexane and dichloromethane (v/v 3:2) as eluent to afford compound **1**. Yield: 40 mg (43%); ^{1}H NMR (300 MHz, $CDCl_3$): δ 7.46 (s, 2H), 7.23-7.21 (d, *J* = 8.4 Hz, 4H), 7.02-6.99 (d, *J* = 8.4 Hz, 4H), 6.77 (s, 8H), 2.40 (s, 6H), 2.26 (s, 12H), 2.03 (s, 24H); ^{13}C NMR (75.5 MHz, $CDCl_3$): δ 193.6, 142.4, 141.0, 139.4, 137.7, 133.6, 132.1, 128.5, 127.6, 125.8, 124.4, 93.2, 91.9, 30.3, 23.4, 21.3; HRMS (ESI): *m/z* calcd for $C_{62}H_{61}O_2B_2S_2$: 923.4294; found: 923.4338 ($M+H^+$).

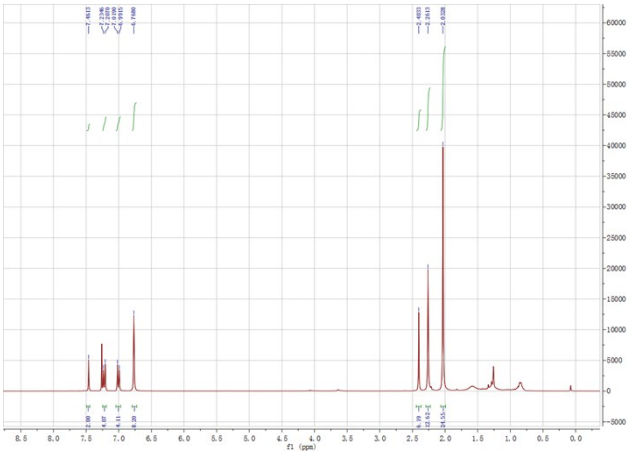

^{1}H NMR spectrum for compound **1**

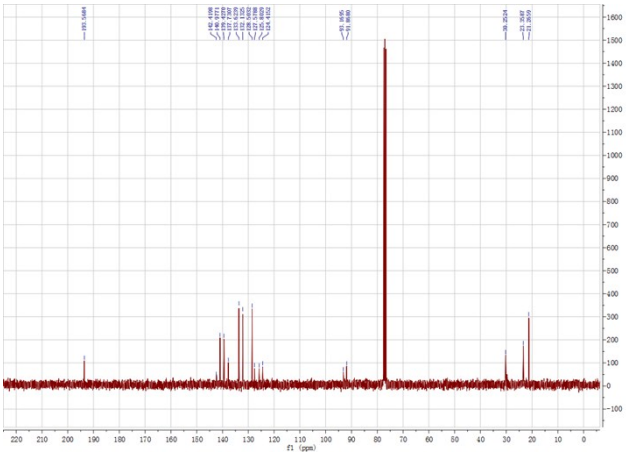

^{13}C NMR spectrum for compound **1**

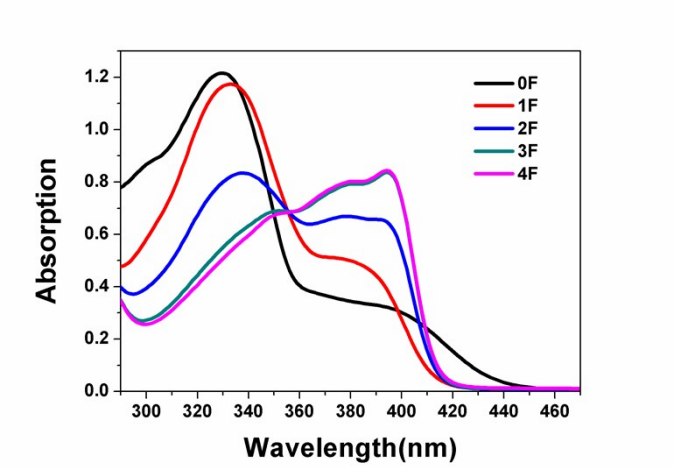

Figure S1 Absorption spectra of **1** in THF:mesitylene (v/v 1:4) (2.0 x 10^{-5} M) at room temperature as a function of molar equivalents of TBAF added.

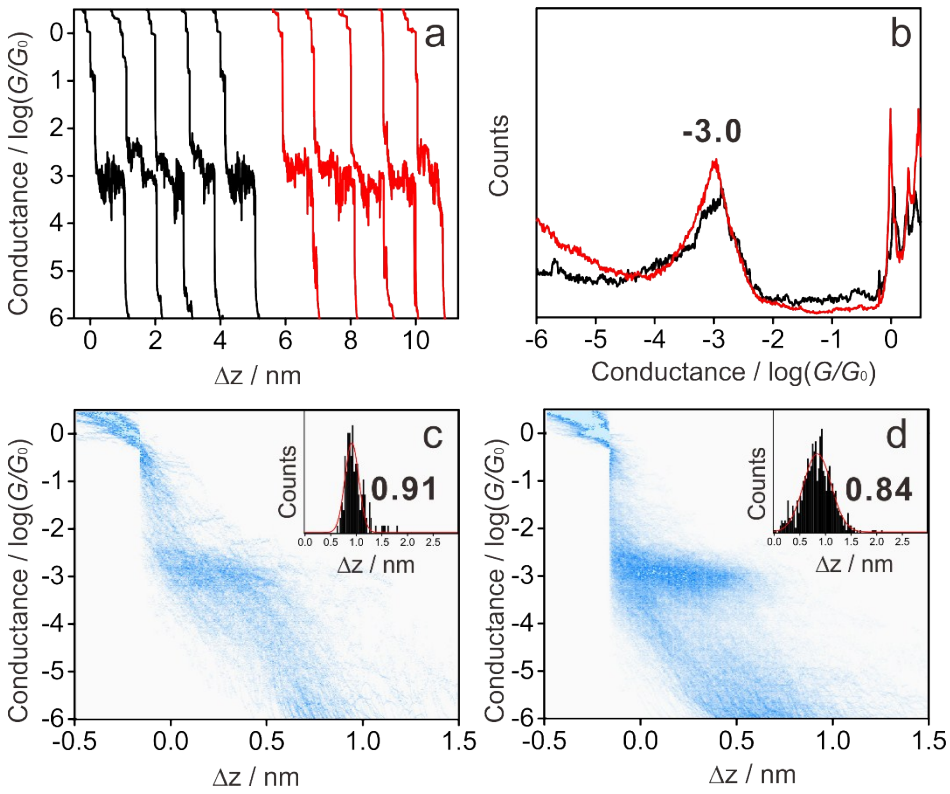

Figure S2. Typical conductance-distance traces (a) and logarithmically binned one-dimensional (1D) histograms (b) of bis[(4-acetylthiophenyl)acetylene in the absence (black) and presence (red) of TBAF recorded during the MCBJ measurements. The conductance of bis[(4-acetylthiophenyl)acetylene is centered at $10^{-3.0}$ G_0. Upon the treatment with TBAF, the conductance remains unchanged. Two-dimensional (2D) histograms and relative stretching distance distributions (inset), for bis[(4-acetylthiophenyl)acetylene in the absence (c) and presence (d) of TBAF.

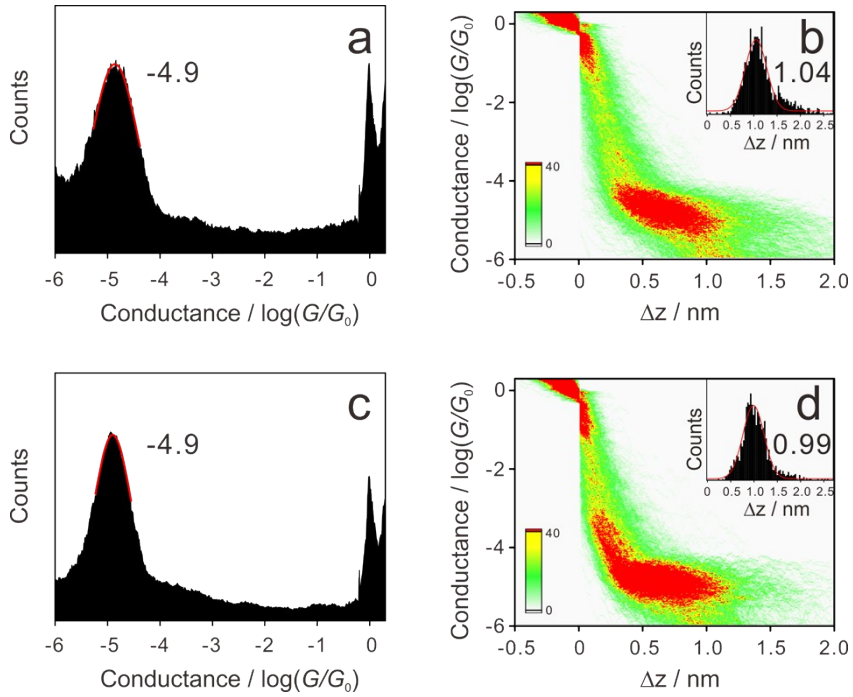

Figure S3. (a) Logarithmically binned one-dimensional (1D) histograms of 1,10-decanedithiol. (b) Two-dimensional (2D) histograms and relative stretching distance distributions (inset) of 1,10-decanedithiol. The conductance of 1,10-decanedithiol is centered at $10^{-4.9}$ G_0 in the absence of TBAF. (c) As shown in the logarithmically binned one-dimensional (1D) histograms of 1,10-decanedithiol the conductance remains unchanged after treatment with TBAF. (d) Two-dimensional (2D) histograms and relative stretching distance distributions (inset) for 1,10-decanedithiol in the presence of TBAF. During the MCBJ measurements, the single-molecule conductance was measured in trimethylbenzene/tetrahydrofuran (4:1, v/v) with the concentration of 1,10-decanedithiol at 0.01 mM and TBAF at 0.04 mM.

2. DFT-based computational methods:

The optimized geometry and ground state Hamiltonian and overlap matrix elements of each structure were self-consistently obtained using the SIESTA[3] implementation of density functional theory (DFT). SIESTA employs norm-conserving pseudo-potentials to account for the core electrons and linear combinations of atomic orbitals to construct the valence states. The generalized gradient approximation (GGA) of the exchange and correlation functional is used with the Perdew-Burke-Ernzerhof

parameterization (PBE),[4] a double-ζ polarized (DZP) basis set, a real-space grid defined with an equivalent energy cut-off of 250 Ry. The geometry optimization for each structure is performed to the forces smaller than 10 meV/Ang. Figures S4a and b show geometry-optimized structures used to obtain the DFT results in Figures 2 and S5. The mean-field Hamiltonian obtained from the converged DFT calculation or a simple tight-binding Hamiltonian was combined with our Gollum quantum transport code to calculate the phase-coherent, elastic scattering properties of the each system consist of left (source) and right (drain) leads and the scattering region. The transmission coefficient $T(E)$ for electrons of energy E (passing from the source to the drain) is calculated via the relation $T(E) = Trace\left(\Gamma_R(E)G^R(E)\Gamma_L(E)G^{R\dagger}(E)\right)$. In this expression, $\Gamma_{L,R}(E) = i\left(\sum_{L,R}(E) - \sum_{L,R}{}^{\dagger}(E)\right)$ describe the level broadening due to the coupling between left (L) and right (R) electrodes and the central scattering region, $\sum_{L,R}(E)$ are the retarded self-energies associated with this coupling and $G^R = \left(ES - H - \sum_L - \sum_R\right)^{-1}$ is the retarded Green's function, where H is the Hamiltonian and S is overlap matrix. Using obtained transmission coefficient ($T(E)$), the conductance could be calculated by Landauer formula ($G = G_0 \int dE\, T(E)(-\partial f/\partial E)$) where $G_0 = 2e^2/h$ is the conductance quantum, $f(E) = \left(1 + exp[(E - E_F)/k_BT)\right)^{-1}$ is the Fermi-Dirac distribution function, T is the temperature and k_B = 8.6×10^{-5} eV/K is Boltzmann's constant.

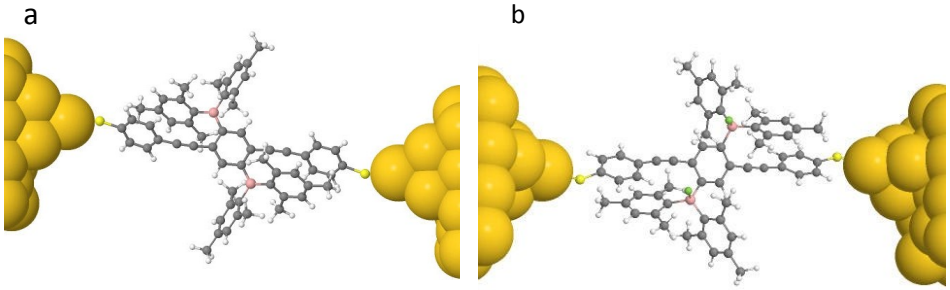

Figure S4. Relaxed structures of molecule a) **1**, b) **1**·2F.

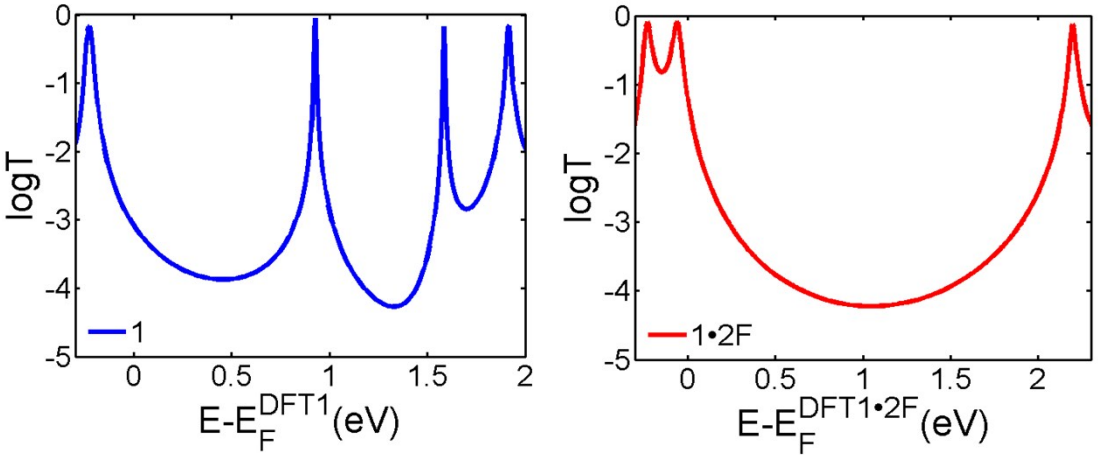

Figure S5. DFT transmission coefficients of molecules **1** (left figure) and **1**·2F (right figure) before gap correction.

The left curve in Figure S5 shows that **1** possesses two transmission resonances at $E - E_F^{DFT1}$ = 0.93 eV and 1.6 eV, and crucially, the right curve shows that these resonances are removed by the attachment of the fluoride. To compare these curves and predict the change in conductance when the fluorides are attached, we need to know the relationship between the experimental Fermi energies E_F^1 and $E_F^{1\cdot 2F}$, which do not necessarily coincide with the DFT-predicted values E_F^{DFT1} and $E_F^{DFT1\cdot 2F}$. The latter will depend on the precise location of the PF_6 counterions, which create a fluctuating environment for **1**·2F. We would also need to perform a scissor correction in the presence of counterions, for which there is no reliable procedure. The experimentally observed conductance ratio of **1** to **1**·2F is approximately 4, which suggests that the DFT estimate for $E_F^{DFT1\cdot 2F}$ is too high. Increasing $E_F^{1\cdot 2F}$ by approximately 0.4 eV yields the transmission curves shown in figure 2 of the main text.

References

1. Giacalone, F., et al., Tetrathiafulvalene-Based Molecular Nanowires. *Chem Commun* **2007**, 4854-4856.

2. Chen, J.; Wenger, O. S., Fluoride Binding to an Organoboron Wire Controls Photoinduced Electron Transfer. *Chem Sci* **2015**, *6*, 3582-3592.

3. Soler, J. M.; Artacho, E.; Gale, J. D.; Garcia, A.; Junquera, J.; Ordejon, P.; Sanchez-Portal, D.,

The Siesta Method for Ab Initio Order-N Materials Simulation. *J Phys: Condens Matter* **2002**, *14*, 2745-2779.

4. Perdew, J. P.; Burke, K.; Ernzerhof, M., Generalized Gradient Approximation Made Simple. *Phys Rev Lett* **1996**, *77*, 3865-3868.